JOURNAL OF CATALYSIS 123, 349–363 (1990)

Mechanistic Studies of Hydrocarbon CH/D_2 Exchange over Thermally Activated Magnesium Oxide

M. FAZLUL HOQ, ILEANA NIEVES, AND KENNETH J. KLABUNDE[1]

Department of Chemistry, Kansas State University, Manhattan, Kansas 66506

Received May 2, 1989; revised December 12, 1989

The CH/D_2 exchange reaction over thermally activated solid base catalyst MgO, where CH represents a hydrocarbon (carbon acid), has been investigated from a mechanistic point of view. Extensive kinetic studies of the exchange, analyses of hydroxyl content of MgO activated at various temperatures, spectroscopic studies, and consideration of pore sizes and possible reaction sites on MgO have led to the following conclusions: (1) the active site on MgO involves basic O^{2-} ions, which abstract protons from carbon acids, as well as acidic Mg^{2+} ions, which stabilize resulting carbanions (2) the active site is probably a defect site of high electron density (perhaps a cation vacancy) and contains an O–H (or O–D) group; (3) the transition state in the R–H(g) + D_2(g) $\xrightarrow{MgO}$ R–D(g) + HD(g) exchange reaction probably involves O^{2-}–D^+ attack on adsorbed R^- --- H^+ in the active site. A reaction coordinate diagram is proposed that explains our findings that exchange rates roughly correlate with literature solution-phase pK_a values for R–H.

INTRODUCTION

From the measured CH/D_2 exchange rates over solid MgO for CH_4, C_2H_6, and methyl and methine CH in isobutane, Tanabe and co-workers concluded,

$$k_{CH_4} > k_{C_2H_6}, \quad k_{HC(C\underline{H}_3)_3} > k_{\underline{H}C(CH_3)_3},$$

that the abstraction of a proton from CH by a basic site on MgO was the rate-determining step, (*1*). Isomerization, amination, and hydrogenation of alkenes and dienes over MgO are also believed to proceed via a proton abstraction step (*2*). The same heterolytic cleavage $RH \rightarrow R^-_{ads} + H^+_{ads}$ over MgO has been proposed by Garrone and Stone (*3*). And our studies of rates of CH/D_2 exchange over MgO have correlated surprisingly well with solution-phase acidity values for R–H carbon acids, and this solid base is capable of controllably removing protons from methane, neopentane, benzene, toluene, and a variety of other hydrocarbons and heterosubstituted hydrocarbons (*4*). All these observations leave little doubt that the cleavage of C–H over active MgO is heterolytic, yielding an adsorbed proton and carbanion. However, little is known about the active sites on MgO involved in this process, or about the C–H activated complex involved. Therefore, we have undertaken a series of experiments intended to offer understanding of this facile exchange process. Thus, a wide range of kinetic analyses of the exchange reaction over various samples of thermally activated MgO were carried out.

$$R\text{–}H_{(g)} + D_{2(g)} \xrightarrow{MgO} R\text{–D} + \text{HD}$$

EXPERIMENTAL

Chemicals

Hydrocarbons were purchased from Aldrich, Fluka, or Columbia Chemicals in their purest form. They were further purified by storage over CaH_2, freeze–thaw degassing cycles, and then passage as a vapor over/through 4-Å molecular sieves held at a temperature just above that at which the

---

[1] To whom correspondence should be addressed.

0021-9517/90 $3.00

hydrocarbon had sufficient vapor pressure. The hydrocarbon was then condensed in a liquid nitrogen trap. As a final purification step the hydrocarbons were passed over thermally activated MgO chips (see below). Finally, the hydrocarbons were stored under vacuum over 4-Å molecular sieves in air-tight sample tubes. Deuterium and hydrogen were purified by passage through 4-Å molecular sieves at −78°C and collected in a 5-liter bulb containing activated (350°C at $<1 \times 10^{-3}$ Torr overnight) 13× molecular sieves.

Magnesium oxide (MgO, 99.999%) from ROC/RIC was treated with deionized distilled water (25 g MgO added to 300 ml boiling water). After boiling and stirring for several minutes, the slurry was hot-filtered by use of a fine porosity glass filter with suction. This hydrated MgO was dried at 110°C for 10 h. The solid mass was broken up into ~2-mm pieces and stored in a sealed glass container. Portions of this MgO were thermally activated as described previously (*4*, *5*).

Reactor

The recirculation reactor employed in these studies is shown in Fig. 1. Catalyst (from 0.04 to 0.1 g) was placed in a quartz U-tube and was thermally activated at 660°C or other desired temperature under vacuum for 3 h. (This tube was cleaned prior to each use with aqua regia, then with KOH–isopropyl alcohol, and finally with deionized distilled water and dried at 120°C for 4 h.)

Hydrocarbon (4 Torr) and D_2 (110 Torr) mixtures were circulated over the activated catalyst at the desired reaction temperature, and samples were extracted periodically into sample tube D′ through stopcock g for GC, MS, or NMR analysis.

Determination of Rate Constants

Deuterium uptake rates were determined by MS analysis, correcting for ^{13}C abundance. The kinetic equation (*6*)

$$C_nH_m(x \text{ Torr}) + D_2(y \text{ Torr}) \xrightarrow{\text{catalyst}} C_nD_m + HD$$

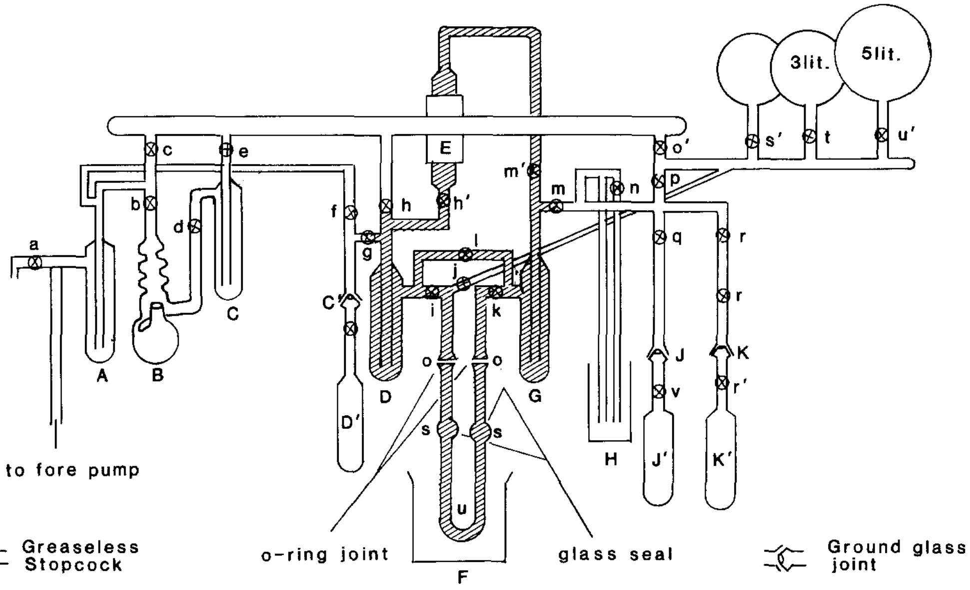

FIG. 1. Schematic of vacuum line and recirculation reactor used in CH/D_2 exchange studies. Stopcocks are shown with lower case letters. Important components are: (A, C) cold trap, (B) diffusion pump, (C and D) cold trap, (D′) sampling tube, (E) magnetically driven piston pump, (U) catalyst container, (F) furnace or cooling bath, (H) manometer; the shaded portion of the vacuum line constitutes the recirculation reactor.

is deduced as follows: Suppose X_i is the percentage of total hydrocarbon molecules present as $C_nH_m-iD_i$ at time t. Then ϕ indicates the number of deuterium atoms present in 100 molecules at time t:

$$\phi = X + 2X_2 + 3X_3 + \cdots + nX_n.$$

If ϕ_∞ is the equilibrium value of ϕ, then the fraction of exchangable H atoms at time t in 100 molecules of hydrocarbon is $(\phi_\infty - \phi)/\phi_\infty$. Provided that all hydrogen atoms in the molecule are equally reactive and isotope effects are negligible, for a first-order exchange the rate $d\phi/dt$ will be proportional to $(\phi_\infty - \phi)/\phi_\infty)$ and the amount of catalyst W:

$$\frac{d\phi}{dt} = k_\phi W\left(\frac{\phi_\infty - \phi}{\phi_\infty}\right).$$

The unit k_ϕ is the number of deuterium atoms entering in 100 molecules per second per unit weight of catalyst.

Integration yields

$$\log(\phi_\infty - \phi) = -\frac{Wk_\phi t}{2.303\phi_\infty} + \log(\phi_\infty - \phi_0),$$

where ϕ_0 is the initial value of ϕ. A plot of $\log(\phi_\infty - \phi)$ vs t is a straight line, the slope of which yields a rate constant according to

$$k_\phi = -\text{slope} \times 2.303 \times \phi_\infty/W.$$

Calculation of Entropy of Activation $\Delta S\ddagger$

In the Arrhenius equation given in Ref. (*7*), $A \exp(-E_a/RT)$, k is the rate constant, E_a is the Arrhenius activation energy, and A is the preexponential factor. For a first-order reaction, A has the same unit as k. A logarithmic form of this equation is $\log k = (-E_a/2.303R)(1/T) + \log A$. Therefore, from a $\log k$ vs $1/T$ linear plot, E_a can be determined from the slope ($= E_a/2.303R$), and A can be determined from the intercept ($= \log A$). From absolute rate theory one can deduce (*7*):

$$A = e^m(C^0)^{1-m} \times (RT/N_Ah) \times e^{\Delta S\ddagger/R},$$

where m is the molecularity of the reaction, C^0 is the standard state of reactants, R is the gas constant, h is Planck's constant, and N_A is Avogadro's number. This can be rewritten as

$$\Delta S\ddagger = R \ln[A(C^0)^{m-1} \times (N_Ah/Re^m)].$$

For a bimolecular reaction, which is the case for CH/D$_2$ exchange over MgO surfaces,

$$\Delta S\ddagger = R \ln[AC^0 \times (N_Ah/RTe^2)].$$

So the value of $\Delta S\ddagger$ depends on the standard state for a bimolecular reaction (*8*). Since CH/D$_2$ exchange occurs only after adsorption of reactants, a reasonable standard state, C^0, must be defined for surface-adsorbed materials. In analogy to the definition of C^0 for three-dimensional matter such as 1 atm at any temperature (T), Kemball and Rideal (*9*) defined a standard state for adsorbed materials in terms of an area per molecule as $22.53T$ Å^2 where T is the absolute temperature. This corresponds to the same volume per molecule as the three-dimensional state if the thickness of the surface layer is 6 Å.

For calculation of $\Delta S\ddagger$, we use

$$k_\phi = Ae^{-E_a/RT}.$$

For a pseudo-first-order reaction, A has the same units as k_ϕ [i.e., No. of D atoms/(100 molecules)$^{-1}$ (g MgO)$^{-1}$ s^{-1}]. The standard state of adsorbed molecules (C^0) defined as an area per molecule and measured by $22.53T$ Å^2 may be calculated at 25°C to be 6.71×10^{-17} m^2. We can replace 1 g MgO by its measured surface area, 129 m^2/g. Now we have

$$AC^0 = A(100)^{-1}\,(129\ \text{m}^2)^{-1}\ \text{s}^{-1} \times 6.71 \times 10^{-17}\ \text{m}^2$$
$$= A \times 5.20 \times 10^{-21}\ \text{s}^{-1}.$$

At 25°C

$$N_Ah/RTe^2 = \frac{6.02 \times 10^{23}\ \text{mol}^{-1} \times 6.63 \times 10^{-34}\ \text{J s}}{8.314\ \text{J K}^{-1}\ \text{mol}^{-1} \times 298\text{K} \times (2.72)^2}$$
$$= 2.18 \times 10^{-14}\ \text{s}.$$

TABLE 1

Entropies of Activation $\Delta S^{\ddagger}$ for CH/D_2 Exchange over Activated MgO

Carbon acid	$\Delta S^{\ddagger}$
Toluene	−27.5
Ethylbenzene	−28.0
Cumene	−28.4
o-Xylene	−26.8
m-Xylene	−27.3
p-Xylene	−27.3
Thiophene	−26.6
Benzene	−26.0
$C_6H_5CD_3$	
ortho-H	−25.9
meta-H	−25.9
para-H	−26.3
$C_6H_5CMe_3$	
ortho-H	−26.1
meta-H	−27.2
para-H	−27.4
CH_4	−26.1
C_2H_6	−26.4
C_3H_8	−25.6
iso-C_4H_{10}	−25.8
neo-C_5H_{12}	−26.4
c-C_3H_6	−26.2
c-C_4H_8	−26.5
c-C_5H_{10}	−26.5
c-C_6H_{12}	−26.5

Now,

$$\begin{aligned}\Delta S^{\ddagger} &= R \ln[AC^0 \times (N_A h/RTe^2)] \\ &= (R/2.303) \log[A \times 5.20 \times 10^{-21}\ \mathrm{s}^{-1} \\ &\qquad \times 2.18 \times 10^{-14}\ \mathrm{s}] \\ &= 0.863(\log A - 33.95)\ \mathrm{cal \cdot mol^{-1}} \\ &\qquad \cdot \mathrm{deg^{-1}}.\end{aligned}$$

Substituting log A values determined from intercepts of log k_{ϕ} vs $1/T$ plots, $\Delta S^{\ddagger}$ values for different CH/D_2 reactions over MgO can be calculated (Table 1).

Measurement of Isotope Effects

(a) ***Primary***. To obtain k_H/k_D for benzylic proton abstraction, toluene and toluene-d_8 were used. Initial exchange rates were compared; that is, only 0.8 to 1.8 atoms D (or H) were incorporated during the kinetic evaluations. Normal reaction conditions were used: 4 Torr toluene, 110 Torr H_2 (or D_2) and 100 and 200°C. The amount of starting MgO was 0.05 g (nonactivated weight). Table 2 summarizes these experiments. It can be seen that reproducibility was very good. Also catalyst reuse experiments showed that poisoning of the catalyst was not a problem. Overall results were k_H/k_D at 100°C = 1.6 and at 200°C = 1.3.

(b) *Secondary*. Relative rates for benzylic exchange in $C_6D_5CD_3$ and $C_6H_5CD_3$ were determined at 100 and 200°C by examining these substrates together: 4 Torr $C_6D_4CD_3$, 4 Torr $C_6H_5CD_3$, 110 Torr H_2. The ratios of rate constants were as follows:

at 100°C
(benzylic exchange $\dfrac{k_D(C_6D_5CD_3)}{k_D(C_6H_5CD_3)} = 1.040$

TABLE 2

Primary Kinetic Isotope Effects for Benzylic Exchange over MgO at 100° and 200°C

Carbon acid	Catalyst[a] no.	Exchange temp (°C)	Rate constant	k_H/k_D[d]
$C_6D_5–CD_3$	1	100	$k_D = 24.3$	$k_H/k_D = \frac{39.3}{24.5}$
	2	100	$k_D = 24.6$	$= 1.604$
$C_6H_5–CH_3$	Reuse of 2	100	$k_H = 39.0^a$	at 100°C
	3	100	$k_H = 39.6$	
	4	100	$k_H = 40.3$	
$C_6D_5–CD_3$	5	200	$k_D = 40.6$	
	6	200	$k_D = 40.0$	$k_H/k_D = \frac{50.9}{40.3}$
	Reuse of 6	200	$k_H = 47.3^b$	$= 1.263$
$C_6H_5–CH_3$	7	200	$k_H = 50.5$	at 200°C
	8	200	$k_H = 51.2$	
$C_6H_5–CD_3$		100	$k_D = 23.6^c$	$k_H/k'_D = \frac{39.3}{23.6}$
		200	$k'_D = 38.1^c$	1.665
				at 100°C $k_H/k'_D = \frac{50.9}{38.1}$ $= 1.336$ at 200°C

[a] The catalyst was activated separately during determination of each rate constant.

[b] k_H values obtained by reusing the catalyst for $C_6H_5–CH_3/D_2$ exchange after pumping out $C_6D_5–CD_3/H_2$ mixture; these k_H values have not been considered during the calculation of average k_H, but are important results demonstrating that $k_D < k_H$ is due to isotope effect, not due to partial poisoning by impurities in $C_6D_5–CD_3$ and/or H_2.

[c] Calculated from experimentally measured ratio $k_D(C_6D_5–CD_3)/k_D(C_6H_5–CD_3)$ and experimental k_D values for $C_6D_5–CD_3$.

[d] No. of isotopes incorporated per molecule ranged from 0.8–1.8 during rate measurements.

at 200°C (benzylic exchange $\frac{k_D(C_6D_5CD_3)}{k_D(C_6H_5CD_3)} = 1.057$ (corrected for some exchange occurring at ring positions).

Thus, a small secondary inverse isotope effect was observed.

Exchange Activity as a Function of MgO Activation Temperature

The rate constant for CH/D_2 exchange in benzene was measured over 0.10 g MgO activated for 6 h at various temperatures (while under vacuum). Reaction temperature was 100°C. From a plot of activation temperature vs k_ϕ (Fig. 2) it appears that maximum activity may be attained by activating at 510 ± 5°C.

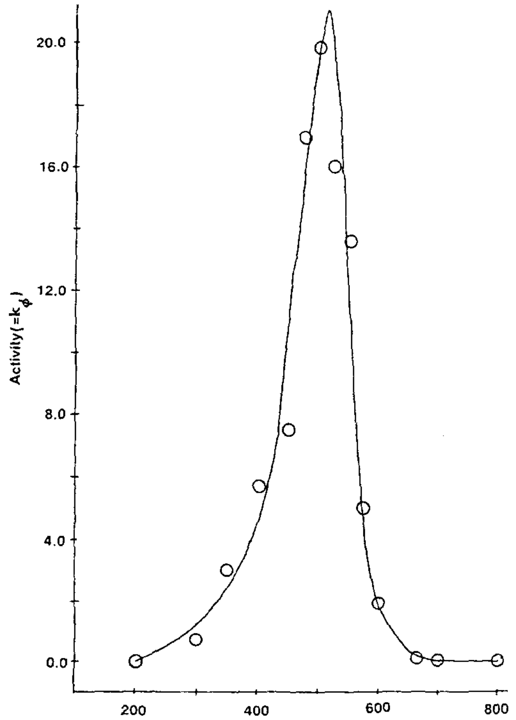

FIG. 2. Relative CH/D_2 exchange rates of benzene over MgO thermally activated at various temperatures (temperature of catalytic reaction = 100°C).

Determination of Residual -OH Groups on Activated MgO

After thermal activation under vacuum, the MgO samples (0.60 g) were cooled to 300°C and treated with 40 Torr pure D_2. In the mass spectrometer the ratio of HD^+ to D_2^+ was determined, and from this information (with known volume of D_2 added), the moles of -OH present on the catalyst could be determined.

NMR Studies of Solid MgO with Adsorbed Carbon Acids

About 1 g of MgO was thermally activated and placed in an NMR tube which was then sealed to a vacuum system. After evacuation the MgO was exposed to an excess of carbon acid at room temperature for several minutes. Excess carbon acid was pumped away and the NMR tube was sealed. Spectra were recorded on the powder using a normal NMR (Bruker WP, 400 MHz for protons). In other words, a "solids" NMR probe was not used. Appropriate blanks were also examined, where the MgO was not exposed to carbon acid. Also, other experiments where the MgO was exposed to H_2 or D_2 were carried out.

Error Limits

By using these experimental methods we were able to determine rather precise values of E_a for each hydrocarbon with possible errors of ±0.02 kcal/mol for more acidic hydrocarbons and ±0.3 for less acidic hydrocarbons. At least three temperatures, usually more, were employed ranging over 100°C; rate constants were measured for each hydrocarbon separately with two to three determinations at each temperature. Error limits did not exceed ±1.6% for k_ϕ for each determination at the same temperature.

RESULTS AND DISCUSSION

Thermal Activation of MgO

First, let us deal with aspects of the MgO surface. It is known that thermal activation of high-surface-area MgO causes the loss of adsorbed water and, depending on temperature, partial loss of surface OH groups (*5*). A defective relatively high-surface-area (usually 120–140 m^2/g) active form of MgO results from this thermal activation step (*5*). The activation is usually done under vacuum between 300 and 1100°C, often around 600°C. The temperature chosen has a dramatic effect on surface activity for subsequent catalytic processes carried out (*10–12*). In this regard, we have made a careful study of thermal activation on activity for CH/D_2 exchange of benzene, and our results are illustrated in Fig. 2. Obviously, there is a dramatic dependence on activation temperature, and about 500°C is optimum (MgO_{500}).

The Question of Pore Size and Restricted Diffusion

It is possible that reaction rates are diffusion controlled, and diffusion could be restricted by pore size. Pore sizes are known for these MgO samples. They range from radii 25–75 Å for a 600°C activated sample (*5*). For our earlier work (*5*) and the present work, the MgO source was a mixture of $MgO/Mg(OH)_2$ (mainly surface-hydroxylated MgO). Upon thermal activation water was desorbed and many hydroxyl groups were eliminated, probably mostly by slight surface reconstruction:

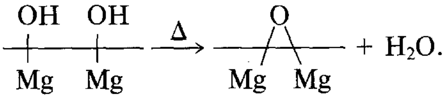

$$\underset{Mg}{\overset{OH}{|}}\!\!-\!\!\underset{Mg}{\overset{OH}{|}} \xrightarrow{\Delta} \underset{Mg\quad Mg}{\overset{O}{\wedge}} + H_2O.$$

Pore size distributions have been studied in more detail by De Vleesschauwer (*13*), where MgO was prepared by $MgCO_3$ decomposition. At 600°C their measured pore size distributions compared well with our results. They also studied MgO activated at 500, 550, 600, 700, and 800°C, and found that average pore radii increased and the distribution broadened with activation temperature increase. Since Fig. 2 clearly shows that exchange rate decreases as temperature of MgO activation goes above 500°C, and since pore sizes increase with higher activation temperature, we believe there is no correlation of reaction rate with pore size, at least for MgO activation temperature above 500°C. (All of our kinetic data in which different hydrocarbons are compared were collected using MgO activated at 660°C.)

On the other hand, we have noted changes in rates and E_a for CH/D_2 exchange in benzene with change in MgO activation temperature (ranging from 5–8 kcal/mol for activation temperatures from 350 to 660°C, the highest E_a found for the highest activation temperature). It has been predicted, on the basis of kinetic arguments, that small restrictive pores would cause a significant decrease in E_a, about halving the true value that would be found with a large-pore unrestrictive catalyst (*14*). Therefore, it is possible that at the lower activation temperature, restrictive pore size may be important. However, about 500°C it seems unlikely, considering the large-pore radii and the data in Fig. 2. We believe a more likely explanation of E_a variation is a change in the nature of the active sites generated by different MgO activation temperatures, rather than due simply to changes in pore sizes. Therefore, on the basis of the relatively large size of these pores, compared with those of RH, and the fact that our rate data do not correlate with pore size change, we believe diffusion through pores is not of rate-determining concern in our experiments (where activation temperatures above 500°C were employed).

Consideration of Steric Factors in Deprotonation

Hoffman and co-workers (*15*) found E_a = 18 kcal/mol for CH/D_2 exchange for both toluene and ethylbenzene in DMSO/*t*-BuO^- suggesting no steric problems in this solution phase system. We found very low E_a values near 1 kcal/mol for toluene, ethylbenzene, and cumene in the $R_H + D_2 \xrightarrow{MgO} RD + HD$ reaction. Since no significant changes in E_a were found for these molecules in our system, this suggests no significant steric problems due to methyl groups, since E_a should be sensitive to steric crowding in the transition state (*16*).

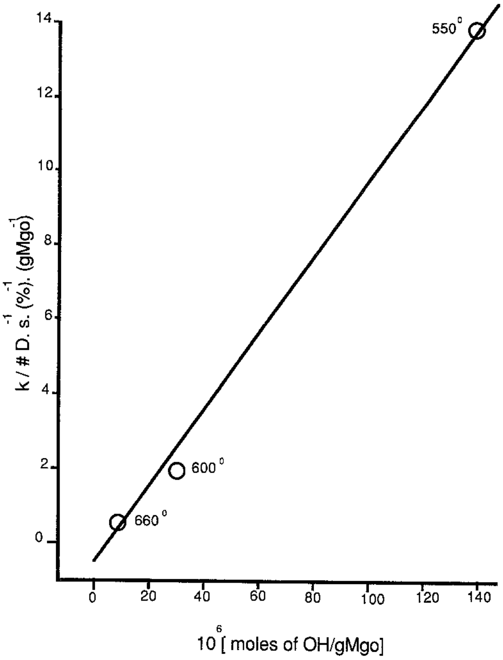

FIG. 3. Plot of OH content vs rate constants for CH/D_2 exchange of benzene over thermally activated MgO.

Role of Surface Hydroxyl Groups

In order to learn more about the nature of these active sites, we determined the hydroxyl content in a series of activated MgO samples. This was done by treating each sample with pure D_2 and measuring the amount of HD formed by means of MS. Activation temperatures of 550, 600, and 660°C were used (*17, 18*), and these yielded 1.38×10^{-4}, 2.89×10^{-5}, and 3.60×10^{-6} mol of OH/g MgO. Our MgO samples have a surface area of 129 m^2/g, so we can calculate the number of OH groups per square nanometer; these results are shown below:

MgO_{550}	0.644 OH/nm^2
MgO_{600}	0.135 OH/nm^2
MgO_{660}	0.017 OH/nm^2

Figure 3 shows a plot of OH content vs rate constants, and there is obviously a good correlation. Also, note that the line in Fig. 3 nearly goes through the origin, supplying more evidence for the need of an OH-bearing site. Such results strongly suggest that an OH group is intimately involved in the catalytically active sites for CH/D_2 exchange. Perhaps this should not be surprising as Boudart and co-workers have reported similar conclusions regarding H_2/D_2 exchange (*19*), and Larson and Hall for CH_4/D_2 exchange over Al_2O_3 samples (*20*). Likewise, Lemberton and co-workers (*21*) concluded that butene isomerizations and H/D exchange in mixtures of protio and deutero butenes depended on the presence of surface OH groups.

In order to define the active site further we can draw on the results of several other literature reports. Molecular orbital calculations have been carried out in a attempt to correlate basicity and surface structure (*22*). Important features in increasing the basicity of certain O^{2-} sites were: (1) low coordination of Mg^{2+} to the O^{2-}, (2) high coordination of nearby O^{2-} to Mg^{2+} adjacent to the O^{2-} in question, and (3) electrostatic interaction between an adsorbed H^+ and the O^{2-} in question. Examples of such low coordination have been symbolized as O^{2-}_{LC} and Mg^{2+}_{LC}, and these are found in surface models of imperfect MgO crystallites given by Coluccia and co-workers (*23, 24*). Such species are also generated by the presence of Schottky and/or Frenkel defects (*5, 12*).

Studies of residual OH on CaO (*25*) have led to the conclusion that basic sites for H^+ abstraction may be adjacent to already existing OH sites, although there also exist non-OH sites capable of H^+ abstraction from benzaldehyde or isopropyl alcohol. In the absence of similar data for MgO, we may recall the study of CO_2 adsorption by Krylov and co-workers (*26*), in which they proposed three types of basic sites on MgO:

(1) strongly basic O^{2-}, (2) strongly basic O^{2-} sites adjacent to OH, and (3) weakly basic surface OH groups.

Thus, our rate data vs OH content and literature precedent lend strength to the idea that the active site contains an -OH moiety. The site is probably very strongly basic as well, since proton abstraction can take place with essentially any hydrocarbons. Also, some NMR data we have collected suggest that the site is rich in electron density. Surprisingly, the resonance for residual H^+ (presumably as some form of OH) comes at 0.0 ppm relative to TMS. Since OH absorptions generally are observed at much lower fields, these data indicate that the residual proton is highly shielded, thus bound to a site of high electron density, (Of course, we cannot be sure that the proton we observe by NMR is in the active site. However, only one absorption was observed, and the kinetic data clearly show that a small amount of residual OH is necessary for high exchange rates; this suggests that the residual OH may be at or very near the true active site.)

Role of Surface Mg^{2+}

We have already discussed the dramatically low activation energies for CH/D_2 exchange over MgO (*4, 27*). Such findings require that a bifunctional catalytic process be operating such that the active site can pull the proton, but simultaneously stabilize/coordinate the carbanion. Thus, the presence of one or more Mg^{2+} in the active site is understood. In addition, we have found that CH/D_2 exchange is very facile over activated MgO for carbon acids in the range 30–60 pK_a. Carbon acids more acidic than that poison the catalyst. This is reasonable considering that carbanions from stronger acids form stronger bonds with magnesium (*28*) and irreversible proton abstraction could thus occur. However, Lewis bases can also poison the catalyst. For example, NH_3 and $C_6H_{11}NH_2$, whose pK_a values (*29, 30*) are in the range of fast exchange (*4*b), only cause poisoning and no NH/D_2 exchange occurs. This finding also requires that a Lewis acid site (i.e., Mg^{2+}) be an intimate part of CH/D_2 exchange site and cycle.

Probing Active Site Structure

The acidities of C–H in furan and thiophene have been examined in DMSO/*t*-BuO^- (*31*). Very large differences in C–H acidities have been recorded in this media, and relative rates of exchange are shown in Table 3; the large rate differences in solution are explainable on the basis of inductive effects of the heteroatom which apparently overcome destabilization of carbanions at the 2,5-positions by heteroatom lone pairs. With thiophene, *d*-orbitals also become important in stabilizing carbanions at the 2 or 5 positions (*31*). So the results in DMSO/*t*-BuO^- are reasonable.

We found, however, that over MgO CH/D_2 exchange rates were almost completely equalized. This was very surprising since hydrocarbons without heteroatoms behaved as expected by their solution acidities (see later discussion (*1–4*). It is clear that the heteroatom-containing substrates are handled much differently by the active sites on MgO.

Since Lewis acid sites are crucial to the exchange process and since furan and thiophene would be expected to behave as Lewis bases through their heteroatoms, we

TABLE 3

Relative Rates of H/D Exchange in Furan and Thiophene in DMSO/*t*-BuO^- Solution and over MgO Surface

DMSO/*t*-BuO^-	MgO Surface
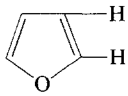 H 0.002 H (1.00)	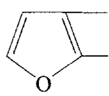 H (1.00) H 1.12
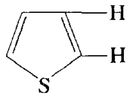 H 0.002 H 500	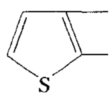 H 1.02 H 1.15

propose that strong complexation of the heteroatom lone pair with Lewis acid sites can explain these acidity-leveling results (reaction (1)). Note that the 3,4-positions could be affected most favorably. So our data strongly imply that a Lewis acid site is an intimate part of the active site. In fact, the Lewis acid site may also help orient furan or thiophene for more efficient interaction with the basic site.

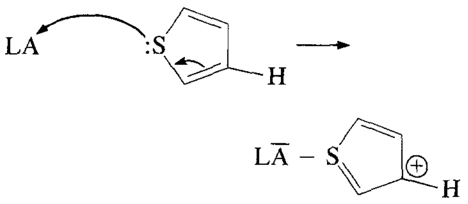

(1)

A little further insight comes from considering hydrogen as a chemical probe. Ito and co-workers (*32*) have studied temperature-programmed desorption of adsorbed H_2 from thermally activated MgO. Interestingly, with MgO_{500} all H_2 was readily desorbed at one time around 110°C. However, MgO_{850} held adsorbed H_2 more tightly; some desorbed about 127°C, more at 230°, 290°C, and a little at 420°C. From our data, MgO_{500} is the most active catalyst for CH/D_2 exchange. This catalyst is, of course, also capable of rapid H_2/D_2 exchange. Now we also know that it easily releases adsorbed, scrambled H_2 (or HD or D_2). If we assume that higher and higher activation temperatures allow more and more dehydroxylated, defective sites to become available, these are the sites that tend to hold H^+_{ads} and H^-_{ads} more tightly.

We also know that not much H_2 is present on the surface at any one time, however, as we could not detect ^1H NMR lines for chemisorbed H^+ or H^- from H_2. Nor did treatment with H_2 cause a buildup of H^+ in CH/D_2 active site. However, D_2 addition did cause the H^+ in the CH/D_2 site to exchange to D^+.

If we assume that dissociation of H_2 occurs on the lowest coordination sites of Mg^{2+} and O^{2-} (i.e., Mg^{2+}_{3C} and O^{2-}_{3C}, where 3C stands for three coordination sites to oxygen or magnesium, 4C for four sites, etc.) and that these sites tightly bind the H^+_{ads} and H^-_{ads}, we could also assume that such corner- or edge-defective sites are not the CH/D_2 exchange sites.

Thus, $Mg^{2+}_{3C}O^{2-}_{3C}$ and $3Mg^{2+}_{3C}2O^{2-}_{5C}$ could be ruled out as exchange sites. We note that the dissociative adsorption of H_2 was attributed to the pair consisting of low-coordinated oxide and magnesium ions (*23*). Toluene is one of the fastest exchanging acids over MgO (*4*). Since H_2 is 6 pK_a units more acidic than toluene (ion-pair pK_a of hydrogen (*33*) = 35.3 ± 0.3 and that of toluene (*34*) = 41.2), we believe that a strongly basic oxide such as O^{2-}_{3C} is not essential for deprotonating hydrogen; a mildly basic oxide (e.g., O^{2-}_{4C}, O^{2-}_{5C}) ion may be good enough to result in the dissociative adsorption of hydrogen provided a highly acidic magnesium (e.g., Mg^{2+}_{3C}) is available to stabilize the hydride.

These considerations argue against the CH/D_2 exchange site being a low-coordination edge or corner site. Thus, there must be some other unique feature. We propose that this feature is possibly a cation vacancy. Such a site would be deeply basic and could strongly adsorb H^+ or D^+, and similar sites have been implicated in earlier work we carried out in which abstraction of H^+ was rate determining (*35*).

Transition State for Exchange

We return to the question of activation energies for exchange. Table 4 compares E_a values for solution studies from the literature and our MgO system. The values for H/D exchange in toluene, for example, are very different and suggest differences in transition states in each system. In DMSO/*t*-BuO a structure such as **1** has been proposed (*15*). Note that the potassium ion does not play a role since it is taken out of the picture by strong DMSO solvation. In contrast, Streitweiser and co-workers (*30*a), on the basis of a great deal of information, have proposed a four-centered

TABLE 4

Arrhenius Activation Energies for Base-Catalyzed Hydrogen Isotope Exchange in Different Systems

Carbon acids	E_a(kcal/mol)		
	DMSO/t-BuO$^-$	CHA/LiCHA	Basic surface of MgO
$C_6H_5C\underline{H}_3$	18^a		0.9
$C_6H_5C\underline{H}_2CH_3$	18^a		0.1
p-$(C\underline{H}_3)_2C_6H_4$	21.6^a		1.1
	NH_3/KNH_2		
Benzene-d	$16.2^{b,c}$		8.9^d
Toluene-α-d		10.0^b	1.7

[a] Ref. (*15*).

[b] The authors reported $\Delta H\ddagger = 8.8$ kcal/mol for toluene (*38*) and 15 kcal/mol for benzene (see footnote *c*); we converted to E_a using the equation $E_a = \Delta H\ddagger + mRT$, where m indicates molecularity (in this case $m = 2$), $R = 1.987$ cal/mol · deg, and $T = 298°K$ (*8*).

[c] Ref. (*31*), page 89.

[d] Experimental E_a(C–H) for benzene = 8.1 kcal/mol; experimental E_a(C–D) − E_a(C–H) for toluene = 1.7 − 0.9 = 0.8 kcal/mol; we therefore, calculate E_a(C–D) for benzene as 8.1 + 0.8 = 8.9 kcal/mol; examples of such calculations have been reported (*38*). (Although E_a can vary with different MgO activation temperatures, we have chosen 8.1 kcal/mol for comparison with toluene derivatives since all these data were collected using MgO activated at the same temperature (660°C).) Then $\Delta H\ddagger$ was calculated from E_a as in footnote (*b*).

transition state in the CHA/LiCHA system (structure **2**), in which ion pairing is very important. Dotted lines in **2** represent bonds that are largely electrostatic in nature. Thus, when $^-NHC_6H_{11}$ begins to pull H^+ away from the carbon acid, the Li^+ counterion starts to form an ion pair with the developing carbanion, and this probably lowers E_a.

In our system we have the most extreme case of ion pairing and low E_a, and the transition state must resemble **3**.

$[R\text{----}H\text{----}B]^-$

1

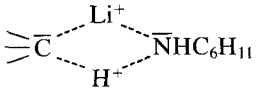

2

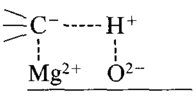

3

So as one might predict, a structure like **3** must be important.

Next, let us consider entropy of activation. We found that for more than 18 carbon acids of widely different structures (benzylic and aromatic C–H, aromatic heterocycles, alkanes and cycloalkanes) the entropies of activation ranged from −25.6 to −28.4 eu (Table 1). The $\Delta S\ddagger$ values were nearly constant, which leads to two conclusions: (1) the large negative values indicate that the surface complex is bimolecular and has a well-arranged and compact structure, and (2) the structure of this complex is nearly the same for all the substrates examined.

The isotope effect $k_H/k_D \approx 1.3$ (at 200°C) indicates that the activated complex has a nearly symmetrical nature such that it has nearly equal chances of decomposition into R–H or R–D.

$$D^{\delta+} \text{ --- } R^{\delta-} \text{ --- } H^{\delta+}.$$

In further discussion of the active site and the activated complex, simplified notations will be used. The active site is simplified below with an O^{2-}, another O^{2-} as an O–D group, and Mg^{2+} as the Lewis acid, as shown below:

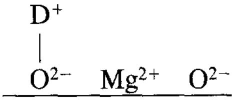

A

We know that the residual O–H exchanges to form O–D in the presence of D_2 or deutero-hydrocarbons. In fact, with D_2, exchange occurs almost instantaneously (*19*).

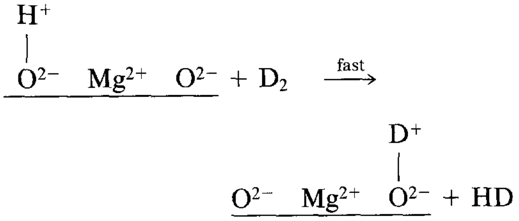

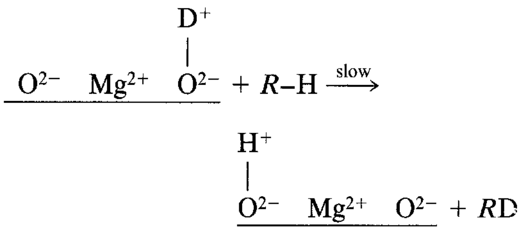

$$\underline{O^{2-}\quad Mg^{2+}\quad \overset{\overset{D^+}{|}}{O^{2-}}} + R\text{–}H \xrightarrow{\text{slow}}$$

$$\underline{\overset{\overset{H^+}{|}}{O^{2-}}\quad Mg^{2+}\quad O^{2-}} + RD$$

We expect that a cycle is set up in which D^+ and D^- are formed and are mobile on the MgO surface.

Table 5 and Fig. 4 show that the rate of heterolytic dissociation of R–H on MgO depends on the acidity of R–H. This correlation with "solution acidities" suggests a transition state for the exchange reaction that resembles neither products nor reactants. (These results also suggest that estimates of pK_a of hydrocarbons may be possible by use of such heterogeneous CH/D_2 kinetic exchange studies and we will report on this later.) This is in accord with our isotope k_H/k_D results. In other words, the transition state is a structure on the path from R–H to R^- + H^+, with the R–H bond greatly perturbed.

In such a structure return to R–H would be slightly more favored than R–D formation, which would agree with the k_H/k_D = 1.3 value (which tells us that internal return is important). Scheme 1 summarizes how we believe the exchange occurs on the active site **A**. The position of the equilibrium, (B) $\rightleftarrows$ (D), Scheme 1) will be dependent on pK_a of R–H. In **E** we have the C–H bond at the limit of weak covalency, and the Mg^{2+} --- R^- interaction is largely of ion-pair type. Attacking D^+ is driven by electrostatic forces, so the species would not be completely symmetric.

TABLE 5

Rates $k_{300°C}$ (k_ϕ Divided by Number of Exchangable Hydrogens) on Logarithmic Scale[a] Obtained from RH + $D_2 \xrightarrow{MgO} R$D + HD Experiment

Carbon acid studied	log $k_{300°C}$ (k_ϕ/Ex.H)	pK_a estimate[b,c]
$C_6H_5C\underline{H}_3$	5.278	(42) 35
$CH_2{=}CHC\underline{H}_3$	4.548	35.5
C_6H_6	3.823	37
$CH_2{=}CH_2$	3.375	36.5
c-C_3H_6	2.533	39
c-C_4H_8	0.666	43
c-C_5H_{10}	0.342	44
c-C_6H_{12}	0.000	(standard) 45
CH_4	1.169	(55) 40
CH_3CH_3	0.114	42
$CH_3CH_2C\underline{H}_3$	0.147	
$(CH_3)_2CHC\underline{H}_3$	0.360	
$(CH_3)_3C\text{-}C\underline{H}_3$	0.446	44

[a] The temperatures employed for CH/D_2 exchange varied from 50° to 300°C, depending on the hydrocarbon under study. These were adjusted to 300°C using experimentally determined activation energies, thus yielding log $k_{300°}$.

[b] Values in parentheses are more recent and more valid determinations (Ref. (*29*)) and Bordwell, F. G., Algrim, D., Vanier, N. R., *J. Org. Chem.* **42,** 1817 (1977).

[c] These values are taken from Cram's MSAD scale (Cram, D., "Fundamentals of Carbanion Chemistry." Academic Press, New York, 1965). These are believed to be in "serious error" (Streitweiser, A., Jr., Juaristi, E., Nebenzahl, L. L., "Equilibrium Carbon Acidities in Solution" *in* "Comprehensive Carbanion Chemistry" (E. Buncel and T. Durst, Eds.), Part A, Chap. 7. Elsevier, New York, 1980.) However, since good estimates of these hydrocarbon acidities are not available, the trends in the MSAD scale are appropriate for the comparisons we want to make here.

The situation can be described further on a reaction coordinate diagram, which is shown in Scheme 2: the R–H physisorbs on the active site **A**, resulting in some loss of translational and rotational freedom (*6*), yielding **B** of Scheme 1. Next, **B** passes through a barrier **C** to give adsorbed R^- and H^+ described by **D**. The barrier to the overall reaction is represented by **E**, and requires the attack of O^{2-}–D^+ in **D**. Then analogous backward steps lead to **F**, **G**, **H**, and finally products. At this point the MgO surface provides adsorbed D^+ and D^- as mobile species, H–D is eliminated, and O^{2-}–D^+ is again available by interaction with deuterium.

Of course, in this scheme the energies of **D** and **H** cannot be too low; that is, the acidities of R–H cannot be too great, or catalyst poisoning will occur. Thus, deep

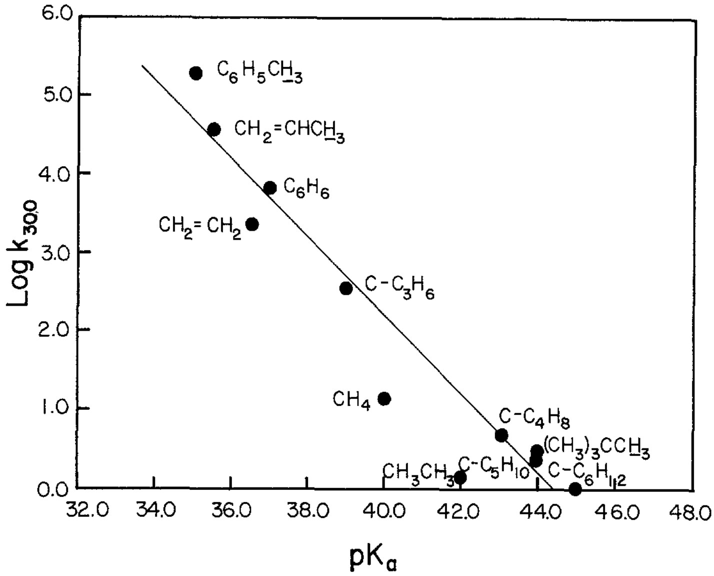

FIG. 4. Plot of the log of the rate constant for CH/D_2 exchange (log k_{300}) for various hydrocarbons (this work) vs literature pk_a estimates (see Table 5).

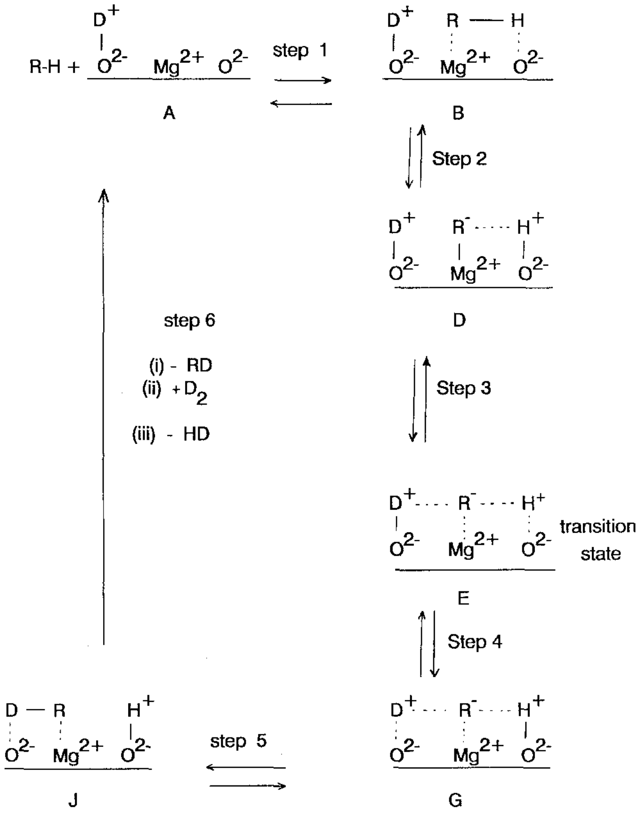

SCHEME 1. Catalytic cycle for exchange of *R*–H with surface OD group.

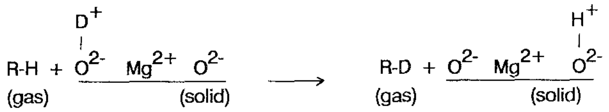

$$\underset{\text{(gas)}}{\text{R-H}} + \underset{\text{(solid)}}{\underline{\overset{D^+}{O^{2-}}\ Mg^{2+}\ O^{2-}}} \longrightarrow \underset{\text{(gas)}}{\text{R-D}} + \underset{\text{(solid)}}{\underline{O^{2-}\ Mg^{2+}\ \overset{H^+}{O^{2-}}}}$$

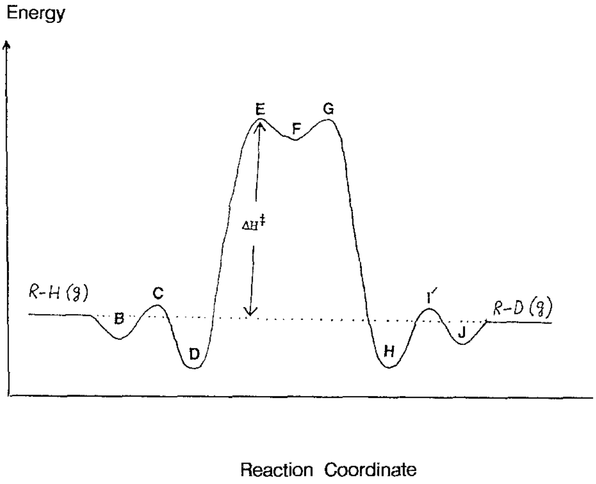

SCHEME 2. Reaction coordinate diagram for *R*H + $D_2 \rightarrow$ *R*HD + HD exchange.

energy wells in **D** and **H** cause irreversible adsorption.

CONCLUSIONS

Overall, our findings and considerations, in summarized form, are enumerated below:

(1) Dramatically low activation energies (E_a) were found.

(2) Kinetic acidities (log of rate constants) correlated with various published solution-phase acidity determinations (Fig. 4). (Interestingly, our earlier work showed that $\Delta H\ddagger$ derived from E_a correlated with published gas-phase acidities for several *R*–H carbon acids) (*27*).

(3) Nearly constant entropies of activation (−27 ± 1 eu) were found for all carbon acids studied.

(4) Equalization of rates of deprotonation of all C–H in furan and thiophene, which are dramatically different from published solution-phase exchange studies, was observed.

(5) A strong dependence of exchange rates on O–H content in the MgO catalyst was found for the 550–660°C MgO activation temperature range. Below about 500°C activation temperature this correlation breaks down; i.e., lower exchange rates occur in spite of much larger O–H surface concentrations. At the lower activation temperatures a variety of surface O–H species are present, including adsorbed water, which could block active sites.

(6) The k_H/k_D primary isotope effect was 1.3–1.6, and a secondary isotope effect less than 6% was found. These results support the idea that in the transition state the C–H bond is not completely broken, but that it is weakened, whereupon D^+ attacks the incipient carbanion (*36, 37*). A small secondary isotope effect supports this simple idea about the transition state; i.e., no inverse

secondary isotope effect was observed (*36*).

(7) Consideration of pore size in MgO samples and its effect on E_a led to the conclusion that pore size is not important in determining rate when MgO activation temperatures above 500°C are employed.

(8) Steric effects surrounding the C–H site do not appear to be very important.

(9) The active site for CH/D_2 exchange must possess a residual OH (or OD) group in or near a defect site of high electron density, possibly a cation vacancy. However, a Lewis acid site is also necessary so that a bimolecular acid–base reaction is involved in the CH/D_2 exchange process.

ACKNOWLEDGMENT

The support of the Army Research Office is acknowledged with gratitude.

REFERENCES

1. Utiyama, M., Hattori, H., and Tanabe, K., *J. Catal.* **53,** 237 (1978).

2. Hattori, H., *Stud. Surf. Sci. Catal.* **21,** 319 (1984).

3. Garrone, E., and Stone, F. S., *in* "Proceedings, 8th International Congress on Catalysis, Berlin, 1984," Vol. 3, pp. 441–452. Dechema, Frankfurt-am-Main, 1984.

4. (a) Hoq, M. F. and Klabunde, K. J., *J. Amer. Chem. Soc.* **108,** 2114 (1986); (b) Hoq, M. F., PhD thesis, Kansas State University, 1988.

5. Morris, R. M., and Klabunde, K. J., *Inorg. Chem.* **22,** 682 (1983).

6. (a) Kemball, C., *in* "Advances in Catalysis" (W. G. Frankenburg, V. I. Komarewsky, and E. K. Rideal, Eds.), Vol. 2, p. 233. Academic Press, San Diego, 1950; (b) Kemball, C., *in* "Advances in Catalysis" (D. D. Eley, P. W. Selwood, and P. B. Weisz, Eds.), Vol. 11, p. 223. Academic Press, San Diego, 1959.

7. Alberty, R. A., "Physical Chemistry," pp. 131, 626. Wiley, New York, 1983.

8. Robinson, P. J., *J. Chem. Educ.* **55,** 509 (1978).

9. Kemball, C., and Rideal, E. K., *Proc. R. Soc. London* **A187,** 53 (1946); also see Ref. (*6*a).

10. Tanabe, K., "Solid Acids and Bases." Academic Press, New York, 1970.

11. Nieves, I., and Klabunde, K. J., *Mater. Chem. Phys.* **18,** 485 (1988).

12. Klabunde, K. J., Hoq, M. F., Mousa, F., and Matsuhashi, H., *in* "Preparative Chemistry Using Supported Reagents" (P. Laszlo, Ed.). Academic Press, New York, 1987.

13. De Vleesschauwer, W. F. N. M., *in* "Physical and Chemical Aspects of Adsorbents and Catalysts" (B. G. Linsen, Ed.), p. 265. Academic Press, New York, 1970.

14. Wheeler, A., *in* "Advances in Catalysis" (W. G. Frankenburg, V. I. Komarewsky, and E. K. Rideal, Eds.), Vol. 3, p. 249. Academic Press, San Diego, 1951.

15. Hofmann, J. E., Muller, R. J., and Schriesheim, A., *J. Amer. Chem. Soc.* **85,** 3000, 3002 (1963).

16. Gould, E. S., "Mechanism and Structure in Organic Chemistry," p. 178. Holt, Rinehart and Winston, New York, 1959.

17. Measurements on MgO samples activated below 500°C are complicated, we believe, by the presence of adsorbed water on the MgO (as opposed to $^-$OH groups). Above the activation temperature of 660°C the OH content was too low to measure accurately.

18. Anderson, P. J., Horlock, R. F., and Oliver, J. F., *J. Chem. Soc. Faraday Trans. 2* **61,** 2754 (1965).

19. Boudart, M., Delbouille, A., Derouane, E. G., Indovina, V., and Walters, A. B., *J. Amer. Chem. Soc.* **94,** 6622 (1972).

20. Larson, J. G., and Hall, W. K., *J. Phys. Chem.* **69,** 3080 (1965).

21. Lemberton, J. L., Perot, G., and Guisnet, M., *J. Catal.* **89,** 69 (1984).

22. Kawakami, H., and Yoshida, S., *J. Chem. Soc. Faraday Trans. 2* **80,** 921 (1984).

23. Coluccia, S., and Tench, A., *in* "Proceedings, 7th International Congress on Catalysis, Tokyo, 1980" (T. Seiyama and K. Tanabe, Eds.).

24. Coluccia, S., Boccuzzi, F., Ghiotti, G., and Morterra, C., *J. Chem. Soc. Faraday Trans.* **78,** 2111 (1982).

25. Iizuka, T., Hattori, H., Ohno, Y., Sohma, J., and Tanabe, K., *J. Catal.* **22,** 130 (1971).

26. Krylov, O. V., Markova, Z. A., Tretiakov, I. I., and Fokina, E. A., *Kinet. Katal.* **6,** 128 (1965).

27. Tanabe, K., Hattori, H., Yamaguchi, T., and Tanaka, T. (Eds.), "Proceedings, Intern. Symp. Acid-Base Catal., Nov. 28–Dec. 1, 1988, Hokkaido, Japan," pp. 105–121. Kodansha VCH, Tokyo 12, Japan, 1989.

28. (a) Salinger, R. M., and Dessy, R. E., *Tetrahedron Lett.* **11,** 729 (1963); (b) Dessy, R. E., Kitching, W., Psarras, T., Salinger, R. M., Chen, A., and Chivers, T., *J. Amer. Chem. Soc.* **88,** 460 (1966).

29. Algrim, D., Bares, J. E., Branca, J. C., and Bordwell, F. G., *J. Org. Chem.* **43,** 5024 (1978).

30. (a) Streitweiser, A., Jr., Van Sickle, D. E., and Reif, L., *J. Amer. Chem. Soc.* **84,** 258 (1962); (b) The pK_a for NH_3 is about 41 while that for toluene is about 42. We assume cyclohexylamine would be between 42 and 45.

31. Reutov, O. A., Beletskaya, I. P., and Butin, K. P., "CH-Acids" (T. R. Crompton, Ed.), pp. 68, 119, 170. Permagon Press, New York, 1978.

32. Ito, T., Sekino, T., Moriai, N., and Tokuda, T., *J. Chem. Soc. Faraday Trans. 1* **77,** 2181 (1981).

33. Buncel, E., and Menon, B., *J. Amer. Chem. Soc.* **99,** 4457 (1977).

34. Streitweiser, A., Jr., and Guibe, F., *J. Amer. Chem. Soc.* **100,** 4532 (1978).

35. Klabunde, K. J., and Matsuhashi, H., *J. Amer. Chem. Soc.* **109,** 1111 (1987).

36. Laidler, K. J., "Chemical Kinetics," pp. 93, 98. McGraw–Hill, New York, 1965.

37. Cram, D. J., "Carbanion Chemistry," p. 28. Academic Press, New York, 1965.

38. Streitweiser, A., Jr., Granger, M. R., Mares, F., and Wolf, R. A., *J. Amer. Chem. Soc.* **95,** 4257 (1973).